Maneuvers automation for agricultural vehicle in headland

C. Cariou, R. Lenain, Benoît Thuilot, T. Humbert, M. Berducat

Maneuvers automation for agricultural vehicle in headland

C. Cariou[1], R. Lenain[1], B. Thuilot[2], T. Humbert[1], M. Berducat[1]

[1] Cemagref, UR TSCF, 24 Avenue des Landais BP 50085, 63172 Aubière France
[2] Clermont Université, Université Blaise Pascal, LASMEA, BP 10448, 63000 Clermont-Ferrand France

christophe.cariou@cemagref.fr

Abstract
This paper addresses the problem of path generation and motion control for the autonomous maneuvers of agricultural vehicle in headland. A reverse turn planner is firstly presented, based on primitives connected together to easily generate the reference motion. Next, the steering and speed control algorithms are considered. To perform accurate path following, the sliding conditions are taken into account with a kinematic model extended with sliding parameters. In addition, predictive actions are developed to anticipate for vehicle steering and speed variations. The capabilities of the proposed algorithms are finally investigated through full-scale experiments. Fish-tail maneuvers are autonomously performed with an experimental mobile robot, and promising results are reported during reverse turn maneuvers with a vehicle-trailer system.

Keywords : guidance system, mobile robot, maneuvers automation

1. Introduction

For many years, researchers and manufacturers have widely pointed out the benefits of developing automatic guidance systems for agricultural vehicles, in particular to improve field efficiency while releasing human operator from monotonous and dangerous operations. Auto-steering systems are becoming common place, and focus on accurately following parallel tracks in the field. However, more advanced functionalities are today required, in particular for headland driving. In fact, the operator must still manually perform maneuvers at the end of each row before reengaging the automatic guidance system on the next path to follow, see Fig 1. In order to benefit of fully automated solutions, and therefore reduce the operator's workload (and even enable to consider driverless agricultural vehicles), the automation of headland driving has to be studied with meticulous care.

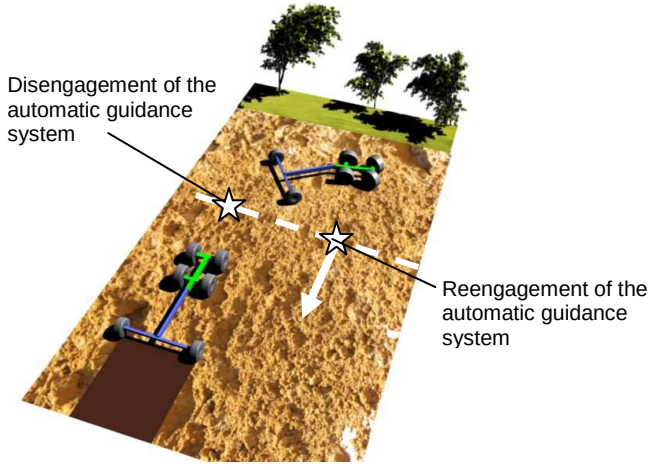

Fig 1: Maneuvers manually performed in headland

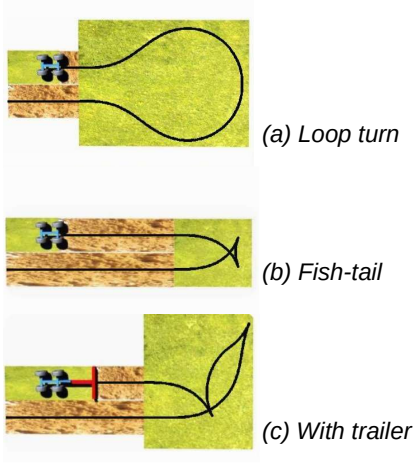

Fig 2: Different types of maneuver

Very few approaches have been proposed in that way, mainly based on loop turns (see Fig 2a) which involve excessive headland width for turning. These approaches are far from optimal, headland being usually low-yield field areas due to high soil compaction or wasted areas as they cannot be used for plantation. This paper proposes to address the reverse turns, *i.e*. maneuvers executed with stop points and reverse motion (see Fig 2b and 2c), leading to reduced headlands, and more in accordance with European agricultural practices.

2. Motion planner

With regard to the path planning problem of agricultural machines in headland, generic optimal control algorithms are often investigated to find optimal point-to-point trajectories for a given cost function from a wide variety of configurations, see [Vougioukas et al. 2006], [Oksanen 2007]. These approaches are based on kino-dynamic models to produce smooth trajectories and demand often excessive computational cost, so that they can hardly be used on-line. In another way, primitive-based planning approaches are widely used in the literature, relying either on clothoids, polynomial splines, cubic spirals or elasticas to construct non-holonomic motions, see [Lau et al. 2006], [Wilde 2009]. We have studied a similar approach well-adapted to agricultural maneuvers. It allows to rapidly obtain an efficient path planning solution for reverse turns of a vehicle-trailer system, based on elementary primitives (line segment, arc of circle) connected together with arcs of clothoid in order to ensure curvature continuity.

The curvature of a clothoid varies linearly with respect to its curvilinear abscissa, see the corresponding shape illustrated in Fig 3a. An arc of clothoid admissible for the considered vehicle can then be defined in order to connect a line segment to a circle of radius R. To avoid the saturation of the steering actuator, R is chosen slightly upper than the minimum curvature radius of the vehicle. The clothoid proportionality coefficient is computed according to the maximum vehicle front-wheel angular velocity and of the vehicle linear velocity during the reverse turn, see [Cariou et al. 2009] for more details. In that way, continuous curvature trajectories admissible for the vehicle can easily be constructed.

The easiest approach consists in generating a fish-tail maneuver, usually performed by self-propelled vehicle or tractor with mounted implement. It is composed of two arcs of clothoid and three arcs of circle, as depicted in Fig 3b. At the stop points, the direction of the wheels are reorientated to change the vehicle rotation instantaneous center.

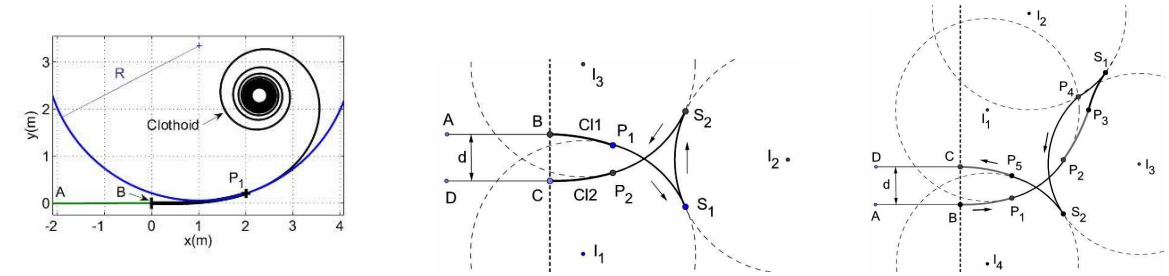

(a) Clothoid *(b) Fish-tail maneuver* *(c) Maneuver with a vehicle-trailer system*

Fig 3: Trajectory generation strategy

If a vehicle-trailer system is considered, the proposed strategy is presented in Fig 3c, and considers the following motions :

- The first movement from B to S_1 is composed of an arc of clothoid BP_1, an arc of circle P_1P_2, a second arc of clothoid P_2P_3, and a part of a third arc of clothoid P_3S_1 required to align the trailer with the vehicle at the end of the movement. Aligning the vehicle-trailer system at the stop point S_1 leads to a suitable configuration to plan the reverse motion.
- The reverse movement is then built, composed firstly of an arc of circle S_1P_4 to increase the vehicle-trailer angle. The point P_4 is determined in order that the center of rotation of the trailer coincides with the center of rotation of the vehicle, when the vehicle front steering angle is set to δ_F=20°, see Fig 4a. Geometrical considerations lead to a vehicle-trailer angle ϕ of 53°. This is a stable configuration enabling a circular motion of radius R. It serves here as an objective configuration. Then, an arc of circle P_4S_2 is built.
- The third movement is composed of an arc of circle S_2P_5 and an arc of clothoid P_5C. S_2 is the second stop point, defined as the intersection between the circles of center I_3 and I_4.

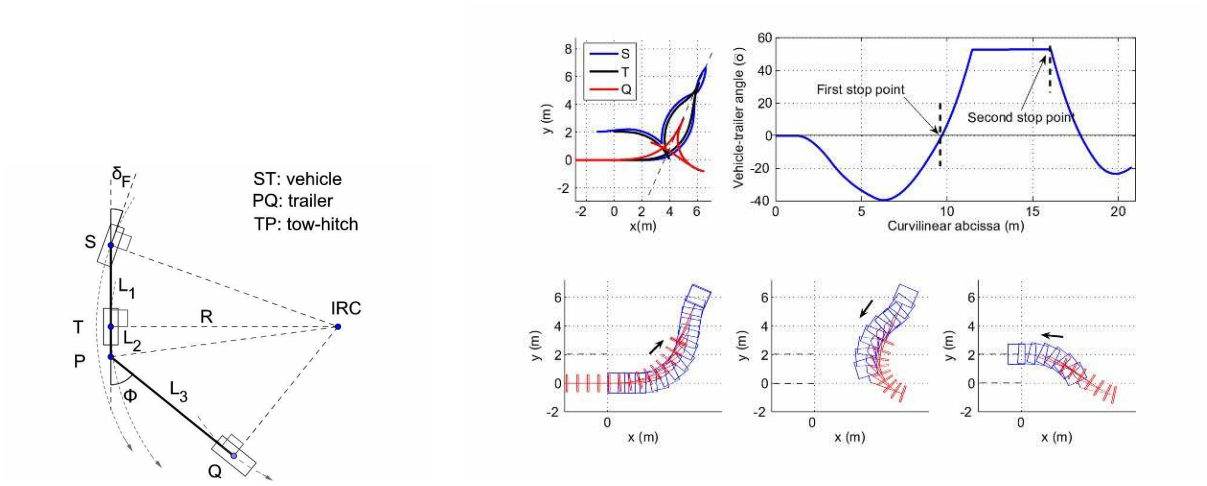

(a) Rotation centers *(b) Path planning results*

Fig 4: Path planning with a vehicle-trailer system

Fig 4b presents path planning simulation results for a vehicle-trailer system with two adjacent tracks separated from a distance d=2m. The vehicle body is represented by a blue rectangle and the trailer by a red one. At the first stop point S_1, the vehicle-trailer angle is ϕ=0°, *i.e.* the trailer and the vehicle are aligned. The trajectories of points S, T and Q, respectively the centers of the vehicle front and rear axle and the center of the trailer axle, are shown in the left-top part of Fig 4b. During the reverse motion, the vehicle-trailer angle ϕ reaches and maintains the expected configuration ϕ_{ref}=53°, as it can be seen in the right-top part of Fig 4b.

Speed reference has also to be associated at each point of the planned trajectories. It is chosen, see Fig 5, in order that the acceleration when commuting from the nominal velocity v_{ref}=1.75m/s to the approaching velocity v_{min}=0.6m/s does not exceed the vehicle maximum longitudinal acceleration a_m=1m/s^2. The approaching velocity v_{min} is 0.6m/s in order to preserve a fast maneuver while obtaining a smooth vehicle stop. The reverse motion is performed at - v_{min} until the system goes past the point P_4, so that the wheels can safely be reorientated from a configuration with I_2 as the instantaneous rotation center to the next one with I_3 as the instantaneous rotation center.

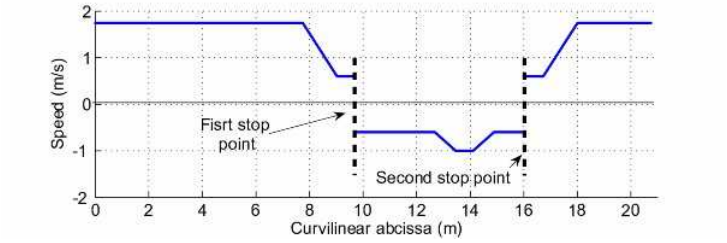

Fig 5: Speed reference

With the motion planner presented in this section, based on geometric primitives connected together and the associated speed reference, fish-tail maneuver for a self-propelled vehicle and the reverse turn maneuver for a vehicle-trailer system are completely defined. The next section presents the control algorithms developed to accurately follow such trajectories.

3. Control algorithms

As the vehicle-trailer system is well-known for being naturally exponentially stable when driving forward, the trailer is ignored in this case. The associated steering and speed control algorithms are described in subsection 3.1. The control specific algorithms for the backward motion are then described in subsection 3.2.

3.1 Forward motion

Accurate automatic guidance of mobile robots in an agricultural environment constitutes a challenging problem, mainly due to the low grip conditions usually met in such a context. In fact, as pointed out in [Wang et al. 2006], if the control algorithms are designed from pure rolling without sliding assumptions, the accuracy of path tracking may be seriously damaged, especially in curves. Therefore, sliding has to be accounted in the control design to preserve the accuracy of path tracking, whatever the path to be followed and soil conditions.

Kinematic model extended with sliding parameters

In the same way than in [Lenain et al. 2006a], two parameters homogeneous with sideslip angles in a dynamic model, are introduced to extend the classical kinematic model, see the bicycle representation of the vehicle in Fig 6. These two angles, denoted respectively β_F and β_R for the front and rear axle, represent the difference between the theoretical direction of the linear velocity vector at wheel centers, described by the wheel plane, and their actual direction. These angles are assumed to be entirely representative of sliding influence on vehicle dynamics. The notations used in this paper are listed below and depicted in Fig 6.

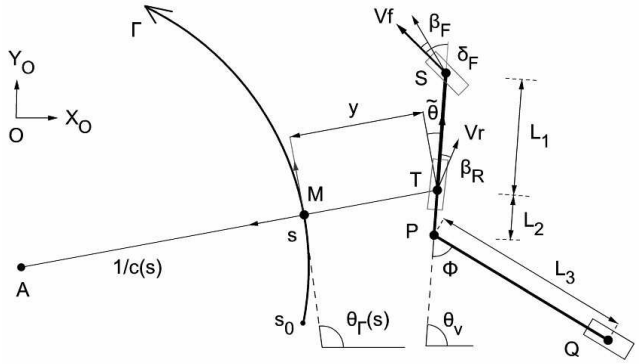

Fig 6: Path tracking parameters

- S and T are respectively the centers of the front and rear virtual wheel. T is the point to be controlled.
- θ_V is the orientation of vehicle centerline with respect to an absolute frame $[O,X_O,Y_O)$.
- δ_F is the front steering angle and constitutes the first control variable.
- V_R is the vehicle linear velocity at point T and constitutes the second control variable.
- β_F and β_R are the front and rear sideslip angles.
- M is the point on the reference path Γ to be followed, which is the closest to T.
- s is the curvilinear abscissa of point M along Γ.
- c(s) is the curvature of the path Γ at point M.
- $\theta_\Gamma(s)$ is the orientation of the tangent to Γ at point M with respect to the absolute frame
- $\tilde{\theta} = \theta_V - \theta_\Gamma$ is the vehicle angular deviation.
- y is the vehicle lateral deviation at point T.
- ϕ is the vehicle-trailer angle.
- L_1=1.2m and L_3=2.34m are respectively the vehicle and trailer wheelbases. L_2=0.46m is the vehicle tow-hitch.

Equipped with these notations, the equations of motion expressed with respect to Γ can be derived as:

$$\begin{cases} \dot{s} &= V_r \frac{\cos(\tilde{\theta}-\beta_R)}{1-c(s)\,y} \\ \dot{y} &= V_r \sin(\tilde{\theta}-\beta_R) \\ \dot{\tilde{\theta}} &= V_r \left[\cos(\beta_R)\lambda_1 - \lambda_2\right] \\ \dot{\phi} &= -\frac{V_r}{L_1 L_3}\left[\tan\delta_F (L_2\cos\phi + L_3) + L_1 \sin\phi\right] \end{cases} \quad (1)$$

$$\lambda_1 = \frac{\tan(\delta_F-\beta_F)+\tan(\beta_R)}{L_1},\ \lambda_2 = \frac{c(s)\cos(\tilde{\theta}-\beta_R)}{1-c(s)\,y}$$

Thanks to estimation of sliding parameters, see our previous work [Lenain et al. 2006b], any variable in model (1) can be known. Therefore, this model constitutes a suitable basis for control design.

Control law design

The control objective is on one hand to perform an accurate path tracking with respect to lateral and angular deviations, and on the other hand to regulate the vehicle velocity on the planned speed reference. In [Lenain et al. 2006a], the first three equations in model (1) have been converted in an exact way into linear equations, according to the following state and control transformations:

$$\begin{aligned} [s, y, \tilde{\theta}] \rightarrow [a_1, a_2, a_3] &= [s, y, (1-c(s)\,y)\tan(\tilde{\theta}+\beta_R)] \\ [V_r, \delta_F] \rightarrow [m_1, m_2] &= [\tfrac{V_r\cos(\tilde{\theta}+\beta_R)}{1-c(s)\,y}, \tfrac{da_3}{dt}] \end{aligned} \quad (2)$$

Finally, if derivatives are expressed with respect to the curvilinear abscissa, the following chained form is obtained:

$$\begin{cases} a_2' &= \frac{da_2}{da_1} &= a_3 \\ a_3' &= \frac{da_3}{da_1} &= m_3 = \frac{m_2}{m_1} \end{cases} \quad (3)$$

Since chained form (3) is linear, a natural expression for the virtual control law m_3 is:

$$m_3 = -K_d a_3 - K_p a_2 \quad (K_p, K_d) \in \Re^{+2} \quad (4)$$

since it leads to:

$$a_2'' + K_d a_2' + K_p a_2 = 0 \quad (5)$$

which implies that both a_2 and a_3 converge to zero, *i.e.* $y \rightarrow 0$ and $\tilde{\theta} \rightarrow \beta_R$. The inversion of control transformations provides then the following front steering control law:

$$\delta_F = \beta_F + \arctan\left\{ -\tan(\beta_R) + \frac{L_1}{\cos(\beta_R)}\left(\frac{c(s)\cos\tilde{\theta}_2}{\alpha} + \frac{A\cos^3\tilde{\theta}_2}{\alpha^2}\right)\right\} \quad (6)$$

$$\begin{cases} \tilde{\theta}_2 &= \tilde{\theta} - \beta_R \\ \alpha &= 1 - c(s)y \\ A &= -K_p\, y - K_d\,\alpha\tan\tilde{\theta}_2 + c(s)\alpha\tan^2\tilde{\theta}_2 \end{cases}$$

In addition, on one hand, as the actuation delays and vehicle inertia may lead to significant overshoots, especially at each beginning/end of curves, a predictive action must be added to the steering control in order to maintain accurate path tracking performances, see [Lenain et al. 2006b] for more details. On the other hand, as the path following performances were demonstrated to be independent from the vehicle velocity, see [Lenain et al. 2006a], a second control loop can be designed, dedicated to speed control. In [Cariou et al. 2009], a Model Predictive Control technique is used to anticipate speed variations and reject signifiant overshoots in longitudinal motion, mainly due to engine delays and inertia. The general principle can be summarized as follows: since the speed reference at each point of the reference trajectory is known, the expected value for the vehicle velocity D_{t+h} after an horizon of prediction h can be inferred from the current position of the vehicle w.r.t. the trajectory.

Then, relying on the actuator model to predict the behaviour of the system, it is proposed to compute a control value C_t with the aim that the actual velocity V_t follows an ideal reference trajectory V^d tending towards D_{t+h}. V^d is classically chosen as a first order dynamic:

$$V_{t+i}^d = D_{t+h} - (D_{t+h} - V_t)\,\lambda^i \quad \text{with} \quad 0 < \lambda < 1 \tag{7}$$

The velocity actuator model was identified as a first order system, with time constant τ=0.42s and gain K=0.97. The model output q at time t+h, when applying constantly control C_t from initial output value V_t, is then:

$$q_{t+h} = V_t e^{-\frac{h}{\tau}} + C_t\,K\left(1 - e^{-\frac{h}{\tau}}\right) \tag{8}$$

The control value C_t ensuring $q_{t+h}= V^d_{t+h}$ can then be deduced from (7) and (8):

$$C_t = \frac{[D_{t+h} - V_t]\left(1-\lambda^h\right) + V_t\left(1-e^{-\frac{h}{\tau}}\right)}{K\left(1-e^{-\frac{h}{\tau}}\right)} \tag{9}$$

3.2 Backward motion

The previous control law (6) can be used to steer backward a self-propelled vehicle, just considering a forward motion with the steering wheels of the vehicle located to the rear. In fact, the first three equations of model (1) describe the motion of such a vehicle, exept that δ_F has to be remplaced by $-\delta_F$, since the variations in the orientation of the vehicle are inverted when rear steering is considered instead of front steering.

In the case of a vehicle-trailer system, It is well-known that steering backward such a system has a tendency to jackknife, and requires special driving skill. In the literature, numerous path following approaches have addressed this problem when the trailer is hooked directly at the center of the rear axle of the vehicle (the standard 1-trailer system). In contrast, the case of deported trailers (the general 1-trailer system) has been rarely considered. In this paper, we propose to indirectly control the vehicle-trailer angle ϕ. Two control strategies are proposed and compared. The first one consists in regulating the vehicle-trailer angle during a part of the backward motion, whereas the second one stabilizes the trailer on the planned trajectory during the whole backward motion. The speed control law for the backward motion is unchanged w.r.t. the forward motion.

Regulation of the vehicle-trailer angle

With the motion planner described in section 2, the previous steering control law (6) can be used during the backward motion until the vehicle-trailer system presents the expected angle ϕ_{ref}, corresponding to the configuration at point P_4 depicted in Fig 4a. Next, as the rest of the backward movement is quite short to reach the stop point S_2, the vehicle-trailer angle can be simply stabilized on ϕ_{ref}. More precisely, relying on the fourth equation in model (1), the error dynamic $\dot{\phi} = K_R(\phi_{ref} - \phi)$, $(K_R > 0)$ can be imposed with the following front-wheel steering control law:

$$\delta_F = \arctan \frac{-L_1 \sin\phi - \frac{K_R L_1 L_3 (\phi_{ref} - \phi)}{V_r}}{L_2 \cos\phi + L_3} \tag{10}$$

Stabilization of the trailer on the planned trajectory

Another solution is to control the center of the trailer axle on its respective planned trajectory. It can be achieved, relying on the following steps:

• The trailer is first considered as an independent virtual vehicle, with a rear steering wheel located at the hitch point P and a fixed front-wheel located at point Q, see Fig 7. The control objective can then be expressed as ensuring the convergence of this virtual vehicle (moving

forward) to the reference path Γ. The first three equations in model (1) describe the motion of such a vehicle, except that δ_F has to be remplaced by $-\delta_C$, since the variations in the orientation of the vehicle are inverted when rear steering is considering instead of front steering. The state variables are now y_t and $\tilde{\theta} = \theta_t - \theta_\Gamma$, respectively the trailer lateral and angular deviation, see Fig 7. A chained form transformation similar to the one presented in subsection 3.1 can then be applied to obtain the value for δ_C.

- δ_C describes the desired direction of the linear velocity $\vec{v}$ at the hitch point. Then, the vehicle-trailer angle ϕ_{ref} ensuring that the center of rotation of the trailer coincides with the center of rotation of the vehicle can easily be inferred from δ_C via basic geometrical relations, see (11) and Fig 7. Finally, the proposed angle ϕ_{ref} can be controlled using (10).

$$\phi_{ref} = \delta_c + \arcsin \frac{L_2 \sin \delta_c}{L_3} \tag{11}$$

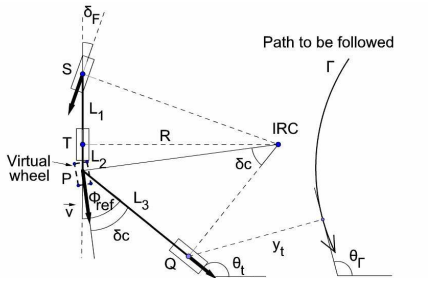

Fig 7: Trailer as a virtual vehicle

4. Experimental results

In this section, the capabilities of the proposed control algorithms are investigated on an irregular natural terrain, using the experimental vehicle-trailer system depicted in Fig 8. The vehicle is an all-terrain mobile robot whose weight is 650kg. The only exteroceptive sensor is an RTK-GPS receiver, whose antenna has been located straight up the center of the vehicle rear axle. It supplies an absolute position accurate to within 2cm, at a 10Hz sampling frequency. The vehicle-trailer angle ϕ is measured using a potentiometer. A gyrometer has also been added to obtain an accurate heading of the vehicle during the maneuvers.

Fig 8: Experimental vehicle-trailer system

4.1 Fish-tail maneuver for self-propelled vehicle

In the forthcoming experimental tests, the track AB is firstly recorded during a preliminary run achieved in manual driving, see Fig 9a. The reverse turn at the end of the track is then automatically calculated with d=-2m, as well as the trajectory back CD. Finally, the path is autonomously followed by the vehicle (without trailer in this case). The lateral deviation according to the curvilinear abscissa is reported in Fig 9b.

At the beginning, the vehicle starts at about 25cm from the path to follow. It reaches then the planned path and maintains (in spite of fast speed and steering variations) an overall lateral error about ±5cm until the first stop point. The reverse motion is also satisfactorily carried out, as well as the back motion, except at the end of the curve with a lateral deviation about 15cm. In fact, the vehicle goes out of the curve at full speed with the front wheels still compensating for the sliding effects during the curve. Although the predictive action reduces significantly overshoots due to actuator delays, the fast variation in the sliding conditions may lead to such overshoots. Therefore, the sideslip angles observer needs to be more reactive. This will demand the integration of dynamic features (center of gravity, moments of inertia, ...) into the observer algorithm, in order to decrease estimation delays and improve accuracy at such transient phase at high speed (to be investigated in future development).

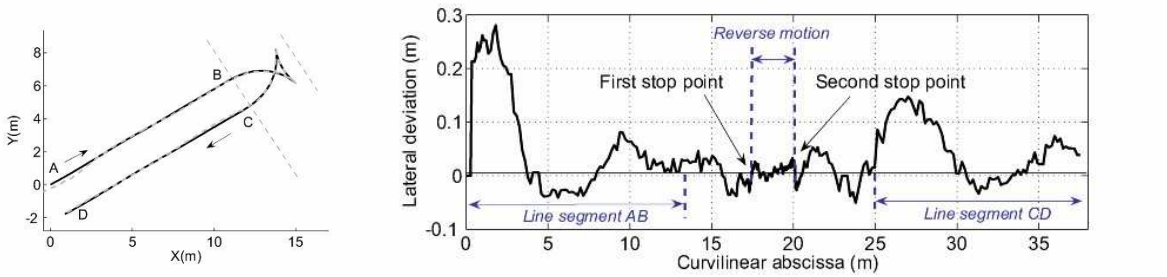

(a) Fish-tail maneuver *(b) Lateral deviation*

Fig 9: Results of the path following

4.2 Maneuver with the regulation of the vehicle-trailer angle

In the forthcoming experimental test, the objective for the vehicle-trailer system is to follow autonomously two straight lines AB and CD separated from 2m, see Fig 10a, and to execute autonomously the reverse turn using control law (10). The lateral deviation recorded at the center T of the rear wheels, according to the curvilinear abscissa, is reported in Fig 10b. At the beginning, the vehicle starts at about 25cm from the path to be followed. Then, it reaches the planned path and maintains an overall lateral error about ±15cm during the maneuver. The main overshoots in the lateral deviation take place at the moment of a large deceleration and acceleration on a sliding ground (curvilinear abscissas 15m and 32m). Despite such conditions, the lateral deviation remains inside ±\pm15cm. This highlights the capabilities of the proposed algorithms, taking into account for sliding effects and actuator delays.

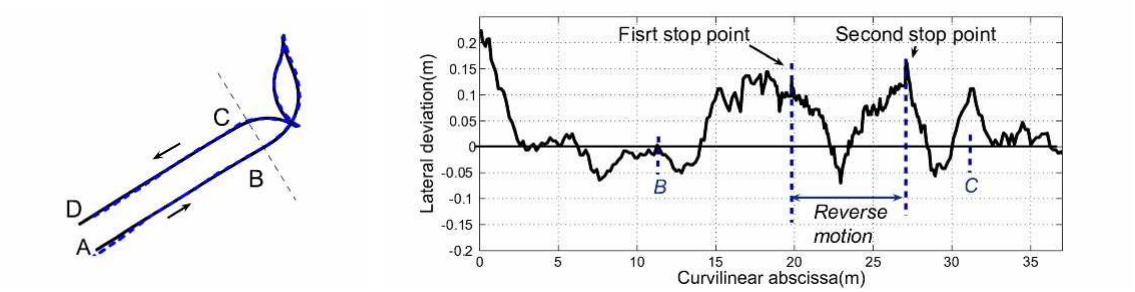

(a) Paths *(b) Lateral deviation at point T (veh. rear axle)*

Fig 10: Results of the path following

The vehicle speed w.r.t. the curvilinear abscissa is reported at the top of Fig 11. The speed reference v_{ref}=1.75m/s is correctly followed, and the speed variations are satisfactorily anticipated with the predictive approach. At the center of Fig 11 is reported the vehicle front

steering angle. It can be observed that its variations are quite smooth and that the wheels are satisfactorily reorientated to change the vehicle instantaneous rotation center at the stop points. The vehicle-trailer angle w.r.t. the curvilinear abscissa is reported at the bottom of Fig 11. In accordance with the simulations depicted in Fig 4b, this angle reaches -40° during the first movement. The trailer and the vehicle are then aligned at the first stop point. During the reverse motion, this angle increases up to ϕ_{ref} =53°. The slight overshoot at curvilinear abscissa 22m is due to the duration of the change in vehicle instantaneous rotation center from I_2 to I_3. The angle is then correctly regulated to the value ϕ_{ref} =53°.

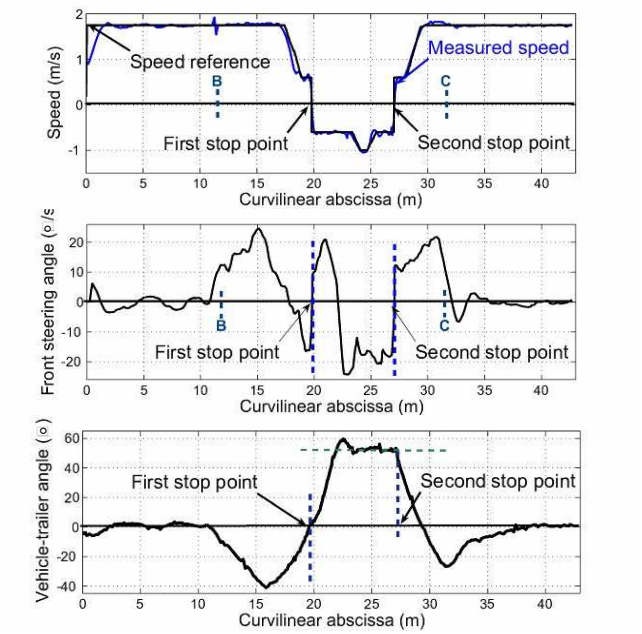

Fig 11: Speed, front steering and vehicle-trailer angle

4.3 Maneuver with the stabilization of the trailer on the planned trajectory

The objective consists first to validate the control law proposed for the stabilization of the vehicle-trailer system on a planned trajectory. To this aim, a 80m-long reference path was first recorded during a preliminary run achieved in manual driving with the mobile robot moving forward, see Fig 12a. Then, the path is autonomously followed backward at 0.5m/s with the vehicle-trailer system. At the beginning, the trailer starts with a lateral deviation of 1m from the path to be followed, see Fig 12b. Then, it reaches the planned path and maintains a satisfactory overall lateral error about ±20cm.

Finally, the reverse turn maneuver depicted in Fig 10a is performed with this control law. The lateral deviation, reported in Fig 12c, maintains an overall lateral error within ±20cm during the maneuver.

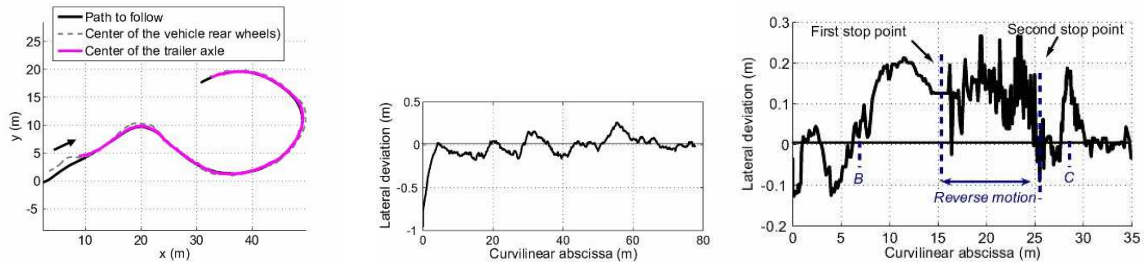

(a) Long reference path *(b) Lateral deviation at Q* *(c) Lateral deviation at Q*

Fig 12: Reversing a vehicle-trailer system

5. Conclusion

This paper addresses the problem of path generation and motion control for the autonomous maneuvers of agricultural vehicle in headland. A motion planner has been first presented, based on primitives connected together with arcs of clothoid, in order to generate admissible trajectories. When the system is driving forward, the control algorithms are based on a kinematic model extended with additional sliding parameters and on model predictive control approaches. When the system is driving backward, different steering controllers have been presented. Promising experimental results are reported with an off-road mobile robot pulling a trailer during reverse turn maneuvers.

In the case of fish-tail maneuver, in spite of fast speed and steering variations required to perform such maneuver, an overall tracking error within ±5cm is obtained, except on the third motion with a punctual lateral deviation about 15cm mainly due the lack of reactivity of the sideslip angles observer. This last point is the object of further development based on the design of mixed kinematic and dynamic observer. In the case of maneuvers with a vehicle-trailer system, an overall tracking error within ±15cm is obtained with the approach regulating only the vehicle-trailer angle. Although this approach requires a dedicated motion planner, it has the main advantage to be very easy to implement and well-suited for short backward motion, such as reverse turn maneuvers. The second approach, stabilizing a vehicle-trailer system on a trajectory, enables to consider longer backward motion during the reverse turn. An overall tracking error within ±20cm is obtained with this approach.

Such headland driving system could be advantageously coupled with a device performing repetitive actions on the farm vehicle (*e.g.* control of the hitches, power take-off, hydraulic valves), enabling to consider full automated solutions. Furthermore, the execution of such maneuvers with a four-wheel steering vehicle and a trailer is currently investigated, on one hand to reduce even more the headland width, and on the other hand to take advantage of explicitely controlling both lateral and angular deviations to perform accurate path following task, see first developments in [Cariou et al. 2008].

References

Cariou C., Lenain R., Thuilot B., Martinet P. (2008). Adaptive control of four wheel steering off road mobile robots: application to path tracking and heading control in presence of sliding. IEEE Int. conf. on Intelligent Robots and Systems, Nice, France.

Cariou C., Lenain R., Thuilot B., Martinet P. (2009). Motion planner and lateral-longitudinal controllers for autonomous maneuvers of a farm vehicle in headland. IEEE Int. conf. on Intelligent Robots and Systems, St Louis, USA.

Lau B., Sprunk C., Burgard W. (2009). Kinodynamic motion planning for mobile robots using splines. IEEE Int. conf. on Intelligent Robots and Systems, St Louis, MO, USA.

Lenain R., Thuilot B., Cariou C., Martinet P. (2006a). High accuracy path tracking for vehicles in presence of sliding: application to farm vehicle automatic guidance for agricultural tasks. Autonomous Robots, 21(1):79-97.

Lenain R., Thuilot B., Cariou C., Martinet P. (2006b). Sideslip angles observers for vehicle guidance in sliding conditions: application to agricultural path tracking task. IEEE conf. on Robotics and Automation, Florida, USA, pp. 3183-3158.

Oksanen T. (2007). Path planning algorithms for agricultural field machines. Research reports 31, Automation Technology Laboratory, Helsinki University of Technology.

Vougioukas S., Blackmore S., Nielsen J., Fountas S. (2006). A two-stage optimal motion planner for autonomous agricultural vehicles. Precision Agriculture, 7:361-377.

Wilde D.K. (2009). Computing clothoid segments for trajectory generation. IEEE Int. conf. on Intelligent Robots and Systems, St Louis, MO, USA.

Wang D., Low C. B. (2006). Modeling skidding and slipping in wheeled mobile robots: control design perspective. IEEE int. conf. on Intelligent Robots and Systems, Beijing, China.